

Efficient Intramolecular General-Acid Catalysis of the Reactions of α -Effect Nucleophiles and Ammonia Oxide with a Phosphate Triester

Anthony J. Kirby,^{*,†} Daniel W. Tondo,[‡] Michelle Medeiros,[‡] Bruno S. Souza,[‡] Jacks P. Priebe,[‡] Marcelo F. Lima,^{†,§} and Faruk Nome^{*,‡}

University Chemical Laboratory, University of Cambridge, Cambridge CB2 1EW, United Kingdom, and Departamento de Química, Universidade Federal de Santa Catarina, Florianópolis, Santa Catarina 88040-900 FT, Brazil

Received November 7, 2008; E-mail: ajk1@cam.ac.uk; faruk@qmc.ufsc.br

Abstract: The $S_N2(P)$ reactions with α -effect nucleophiles of the cationic form $1\cdot H^+$ of phosphate triester diethyl 8-(*N,N*-dimethylamino)-1-naphthyl phosphate are catalyzed by the neighboring dimethylammonium group, with accelerations as high as 10^6 . Hydroxylamine and its *N*-methyl and *N,N*-dimethyl derivatives, which react through oxygen, we presume by way of the zwitterionic ammonia oxide tautomers, are of special interest. The α -effect and the efficient general-acid catalysis in this system are mutually reinforcing. The α -effect is greater for the reactions of the triester than for the corresponding mono- and diesters and qualitatively different for hydroxylamines $RR'NOH$, where the likely role of the ammonia oxide tautomer $NH_3^+-O^-$ is evaluated by ab initio calculations. The initial phosphorus-containing product $NH_2OPO(OEt)_2$ reacts further with hydroxylamine to generate diethyl phosphate and diimide, identified by its disproportionation to hydrazine and N_2 and its reducing potential.

Introduction

We have shown that the hydrolysis of diethyl 8-(*N,N*-dimethylamino)-1-naphthyl phosphate (**1**) is catalyzed below pH 6 by the neighboring dimethylammonium group (Scheme 1, $1\cdot H^+$), with a rate acceleration, compared with that of diethyl 1-naphthyl phosphate, of almost 10^6 .¹ The effective pK_a of the naphtholate leaving group is reduced from 9.4 to 3.4 by partial protonation in the transition state (TS), and the reaction is further catalyzed by oxyanion nucleophiles. A common nucleophilic mechanism, enhanced by general-acid catalysis (GAC) involving the neighboring dimethylammonium group (Scheme 1), accounts satisfactorily for all the observed reactions.¹

More extensive studies of the reactions with nucleophiles of phosphate di- and monoesters **3**² and **4**³ (Scheme 2) have revealed systematic differences compared with the same reactions of similar esters without general-acid catalysis, which are too slow to measure directly in the absence of activated leaving groups. In particular, the neighboring dimethylammonium group makes a strong intramolecular hydrogen bond to the leaving group oxygen in the reactant, as shown by its enhanced pK_a values in the diester **3** $\cdot H^+$ and especially the monoester **4** $\cdot H^+$ (Scheme 2). A significant consequence is that the phosphate

monoester dianion (PO_3^{2-}) group of **4** $\cdot H^+$ is reactive toward oxyanion nucleophiles.³ The pK_a of the dimethylammonium group of **1** $\cdot H^+$ (Scheme 1), by contrast, is close to that expected for an aromatic amine, indicating that intramolecular hydrogen bonding is weak or absent. Nevertheless, intramolecular general-acid catalysis is at least as efficient in the triester, raising intriguing questions about the timing of the proton transfer involved in one of the very few model systems to show highly efficient GAC.^{1,4,5}

Sensitivity to the basicity of the nucleophile, as measured by the Brønsted coefficient β_{nuc} , is typically low for attack on the monoester **4** H^+ , higher for attack on the diester **3** H^+ , and higher still for attack of oxygen nucleophiles on the triester.¹ Most reactive of all near pH 7 are α -effect nucleophiles and in particular hydroxylamines $RR'NOH$ ($R, R' = H$ or alkyl), which show the enhanced reactivity characteristic of α -effect nucleophiles, despite, we suggest,⁶ reacting through their zwitterionic forms $RR'NH^+-O^-$. We report new results for the reactions of triester **1** $\cdot H^+$ with hydroxylamine and its *N*-methyl and *N,N*-dimethyl derivatives, new evidence for oxygen attack by hydroxylamine, and further insight into the mechanisms of these reactions based on these experimental results and ab initio calculations.

Experimental Section

General Procedures. Organic solvents were carefully dried and synthetic reactions carried out in strictly anhydrous conditions under

[†] University of Cambridge.

[‡] Universidade Federal de Santa Catarina.

[§] Present address: Departamento de Química, Universidade Federal de Mato Grosso, Barra do Garças, Mato Grosso 78698-000 MT, Brazil.

(1) Asaad, N.; Kirby, A. J. *J. Chem. Soc., Perkin Trans. 2* **2002**, 1708–1712.

(2) Kirby, A. J.; Lima, M. F.; da Silva, D.; Roussev, C. D.; Nome, F. *J. Am. Chem. Soc.* **2006**, *128*, 16944–16952.

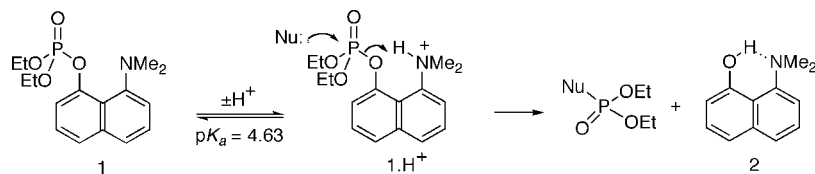
(3) Kirby, A. J.; Dutta-Roy, N.; da Silva, D.; Goodman, J. M.; Lima, M. F.; Roussev, C. D.; Nome, F. *J. Am. Chem. Soc.* **2005**, *127*, 7033–7040.

(4) Hartwell, E.; Hodgson, D. R. W.; Kirby, A. J. *J. Am. Chem. Soc.* **2000**, *122*, 9326–9327.

(5) Kirby, A. J. *Acc. Chem. Res.* **1997**, *30*, 290–296.

(6) Kirby, A. J.; Davies, J. E.; Brandao, T. A. S.; da Silva, P. F.; Rocha, W. R.; Nome, F. *J. Am. Chem. Soc.* **2006**, *128*, 12374–5.

Scheme 1. Outline Mechanism for the Exceptionally Efficient Intramolecular General-Acid Catalysis of the Attack of Nucleophiles on the Phosphate Triester $1 \cdot \text{H}^+$

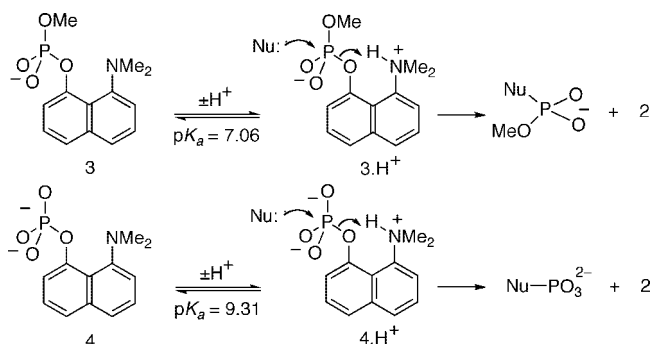


argon. Diethyl 8-(*N,N*-dimethylamino)-1-naphthyl phosphate was prepared as previously described¹ and its structure confirmed by ¹H and ³¹P NMR and by ESI/MS recorded using a Fisons Instrument VG Platform II (a low-resolution instrument). Hydroxylamines (as their hydrochlorides), other nucleophiles, and inorganic salts were of the highest purity available and were used as purchased. For the intermediate trapping experiments ¹H NMR spectra were recorded in D₂O on a Varian Mercury Plus 400 MHz instrument operating at 400 and 162 MHz using sodium 3-(trimethylsilyl)propionate (TSP) as the internal reference for ¹H and 85% phosphoric acid as the external reference for ³¹P, respectively. Chemical shifts are reported as δ (ppm). Mass spectrometry was performed on a Shimadzu GCMSQP5050A instrument operating with a DB5 column (Agilent) with He as the carrier gas. The injector and interface temperatures were kept at 280 and 300 °C, respectively, and the oven temperature was kept for 5 min at 80 °C and then raised, with a constant rate of 10 °C/min, to 300 °C for 5 min. UV spectra were obtained using a Varian Cary 50 diode-array spectrophotometer.

Kinetics. Reactions were initiated by adding 15 μL of a stock solution of the substrate (5×10^{-3} M in acetonitrile) to 3 mL of reaction mixture containing a large excess (0.1–0.5 M) of the nucleophile, thus assuring strictly first-order kinetics for the reaction with the substrate. The kinetics were followed, at 60 °C and an ionic strength of 1.0 M (KCl), for at least 5 half-lives by monitoring the disappearance of the triester **1** at 330 nm on a Varian Cary 50 spectrophotometer equipped with a thermostated cell holder. The pH values of the reaction mixtures were measured at 60.0 °C at the end of each run using a Hanna Instruments model pH 200 pH meter. Observed first-order rate constants (k_{obsd}) were calculated by nonlinear least-squares fitting of the absorbance vs time curve using the Scanning Kinetics WinUV program of the Cary 50; correlation coefficients were 0.998 or better. Second-order rate constants were obtained by linear regression analysis from the slopes of plots of observed first-order rate constants against the concentration of the nucleophile. Hydroxylamines, with the significant exception of methoxyamine, MeONH₂, show the enhanced reactivity expected for α -effect nucleophiles. The pK_a values used for the hydroxylamines at 60 °C are kinetic, derived from the pH–rate profiles of their reactions. Solutions of hydroxylamine nucleophiles were self-buffered between pH 5.5 and pH 7.0 (standard aqueous KOH (0.1 M, Merck) was added to aqueous solutions of hydroxylamine hydrochloride). Other buffers used were HCl/KCl (pH < 2), chloroacetate (pH 2.0–3.5), formate (pH 3.0–4.0), acetate (pH 4.0–5.5), phosphate (pH 5.5–7.0), bis-Tris (pH 7.0–9.0), and borate (pH 8.0–9.0). Data from kinetic measurements are summarized in Tables S.1–3 of the Supporting Information.

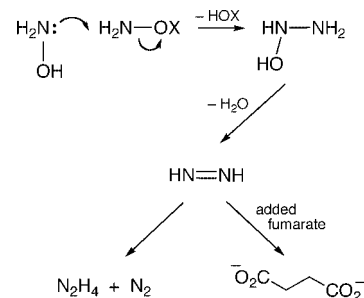
Products of the Reaction. The change in the UV spectrum during reaction shows, as described previously,¹ that the triester is converted quantitatively to 8-(*N,N*-dimethylamino)-1-naphthol (**2**), the expected result of nucleophilic displacement from the phosphorus center of the protonated triester (Scheme 1). The phosphorus-containing product of the spontaneous hydrolysis of $1 \cdot \text{H}^+$ is diethyl phosphate, as expected, but so too, unexpectedly, is the product from the reaction with hydroxylamine. It turns out that the initial product rapidly (we could detect no intermediate in careful NMR experiments) reacts further with the excess hydroxylamine in the solution. Additional products are nitrogen gas and hydrazine: the formation of hydrazine is suppressed by added fumarate, which is

Scheme 2^a



^a The pK_a of the intramolecular general acid increases dramatically over the series triester $1 \cdot \text{H}^+$ < diester $3 \cdot \text{H}^+$ < monoester $4 \cdot \text{H}^+$, while the catalytic efficiency remains high.

Scheme 3^a



^a Hydroxylamine derivatives NH_2OX , where XO^- is a good leaving group (e.g., sulfate¹³ or, in $\text{NH}_2\text{OPO}(\text{OEt})_2$ (**5**), diethyl phosphate), react with hydroxylamine to generate hydroxyhydrazine, which is rapidly dehydrated to diimide (diazene).¹⁴ When the reaction is run in D₂O, exchangeable NH protons are replaced by deuterons and the succinate is produced as $^- \text{O}_2\text{C}-\text{CHD}-\text{CHD}-\text{CO}_2^-$.

itself reduced to succinate by the reactive intermediate involved in the reaction (see the discussion and Scheme 3).

Hydrazine Trapping. N₂H₄ was identified by the formation of the hydrazone with *p*-(dimethylamino)benzaldehyde using the color reagent described by Watt and Chrisp.⁷ Hydroxylamine (Aldrich, 98%) and *p*-(dimethylamino)benzaldehyde (Aldrich, 98%) solutions were prepared using distilled water. A 50 μL volume of a 0.01 M solution of the phosphate triester **1** in acetonitrile was added to 1 mL of a 0.5 M hydroxylamine solution at pH 6.00. After the resulting solution was stirred for 1 h at 25 °C, an aliquot (100 μL) of the reaction mixture was added to 2 mL of the freshly prepared color reagent. The product *p*-(dimethylamino)benzaldehyde hydrazone was identified by its UV–vis spectrum ($\lambda_{\text{max}} = 454$ nm, $\epsilon = 59\,000$ M⁻¹ cm⁻¹⁸). A control experiment, using a solution prepared by the same procedure but without the triester, gave no significant absorbance at 454 nm.

Intermediate Trapping. Under the same conditions, a mixture consisting of 50 μL of a 0.01 M solution of the phosphate triester in acetonitrile was added to 1 mL of a 0.5 M hydroxylamine solution

(7) Watt, G. W.; Chrisp, J. D. *Anal. Chem.* **1952**, *24*, 2006–2008.

(8) Yagil, G.; Anbar, M. *J. Am. Chem. Soc.* **1962**, *84*, 1797–1803.

at pH 6.00 also containing fumaric acid (0.2 M, Carlo Erba, 99.5%, used as supplied). After reaction was complete, an aliquot (100 μ L) was added as before to 2 mL of the same *p*-(dimethylamino)benzaldehyde solution as used above: the UV-vis spectrum showed no significant absorbance at 454 nm.

Identification of Succinic Acid. The succinic acid produced by the reduction of added fumaric acid was identified by ^1H NMR and by mass spectroscopy for reactions involving both the diethyl ester $\mathbf{1}\cdot\text{H}^+$ and the corresponding dimethyl phosphate ester. ^1H NMR experiment: A 1 mL portion of a self-buffered D_2O solution containing 7.0 mg of hydroxylamine hydrochloride and fumaric acid (22.9 mg, a large excess), brought to pD 6.0 by the addition of small aliquots of NaOD, was added to 4.5 mg of $\mathbf{1}$ (4.0 mg for the corresponding dimethyl ester). After the resulting solution was stirred overnight under argon, the ^1H NMR spectrum was recorded, and the succinate signal (δ 2.36, s, 4H) was identified in both cases. (For details see the Supporting Information.) Mass Spectrometry: A 1 mL portion of the product mixture used in the NMR experiment was extracted with 10 mL of ethyl acetate to remove the naphthol. After phase separation, 1 mL of 1 M HCl was added and the aqueous layer again extracted with 10 mL of ethyl acetate to remove organic acids. The organic phase was then dried under argon and the oily residue derivatized by the addition of 30 μ L of *N,O*-bis(trimethylsilyl)trifluoroacetamide to increase the volatility and decrease the polarity of the acids. This mixture was incubated at 80 $^\circ\text{C}$ for 1 h, dissolved in chloroform, and analyzed by GC-MS. The chromatograms show peaks corresponding to the trimethylsilyl derivatives of succinic and unreacted fumaric acid, as well as diethyl (or dimethyl) phosphate (see the Supporting Information). The fragmentation patterns match those from a mixture of authentic samples: except that the fragments from the succinic acid derivative are 2 mass units heavier because in D_2O near its $\text{p}K_{\text{a}}$ the NH protons of hydroxylamine exchange for solvent deuterium (see Scheme 3).

Computational Methods: Geometry Search. Equilibrium structures for reactants, the transition state, and products were obtained using the 6-31G(d,p) basis set at the Hartree-Fock (HF) level, applying the conductor-like polarizable model (C-PCM) during gradient minimization for adding an aqueous-like environment to the system. The resulting structural data (Cartesian coordinates) are summarized in Tables S.4–S.6 of the Supporting Information.

Results and Discussion

Reactions with Hydroxylamines. α -Effect nucleophiles are of special interest because of their high reactivity toward phosphorus, which makes them potential reagents of choice for the deactivation of organophosphorus poisons and chemical warfare agents.⁹ Hydroxylamine is also of particular mechanistic interest because it is known to react with phosphate mono- and diester phosphorus through oxygen, rather than through its more basic nitrogen center.^{10,11} Thus, the reactions of hydroxylamine with the mono- and diesters $\mathbf{4}\cdot\text{H}^+$ and $\mathbf{3}\cdot\text{H}^+$ give the hydroxylamine *O*-phosphates $\text{NH}_2\text{OPO}_3^{2-}$ and $\text{NH}_2\text{OPO}_2^-(\text{OMe})$ (cf. Scheme 2), so the triester would be expected to give $\text{NH}_2\text{OPO}(\text{OEt})_2$. In fact, the phosphorus-containing product observed when reaction is complete is diethyl phosphate. Further investigation showed the presence of an additional product, which was identified

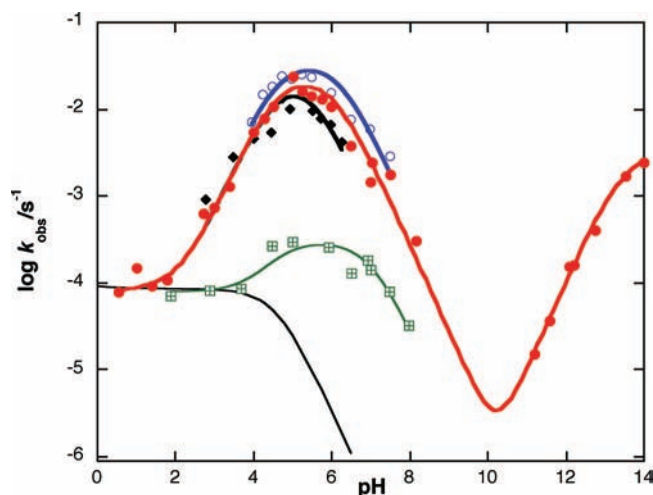


Figure 1. pH-rate profiles (in water at 60 $^\circ\text{C}$ and an ionic strength of 1 M) for the reactions of $\mathbf{1}$ with NH_2OH (filled circles), MeNHOH (open circles), and Me_2NOH (tilted squares). The rate profiles for hydrolysis (curve only)¹ and for the reaction catalyzed by imidazole (squares, this work) are included for comparison. The points are experimental (for data see Table S.1, Supporting Information) and the curves calculated according to eq i, using known values¹ of k_0 (extended to higher pH for NH_2OH by the addition of an anion term) and the substrate $\text{p}K_{\text{a}}$.

as hydrazine. Hydrazine and nitrogen are the known disproportionation products, in aqueous solution under the conditions of our experiments,¹² of diimide, $\text{HN}=\text{NH}$. Evidently, $\text{NH}_2\text{OPO}(\text{OEt})_2$ ($\mathbf{5}$), unlike the products $\text{NH}_2\text{OPO}_3^{2-}$ and $\text{NH}_2\text{OPO}_2^-(\text{OMe})$ of the reactions of hydroxylamine with phosphate mono- and diesters, has a good enough leaving group in diethyl phosphate to react rapidly with the large excess of hydroxylamine present as shown in Scheme 3, thus triggering the series of reactions involved in the formation of the highly reactive diimide intermediate. Diimide is known to be a powerful reducing agent, and its presence in the reaction is confirmed by a supplementary experiment run in the presence of fumarate, which suppresses the formation of hydrazine and is reduced under the conditions to succinate. This series of reactions (which we have observed also with the neutral triester diethyl 2,4-dinitrophenyl phosphate¹⁵) is powerful evidence for nucleophilic attack by hydroxylamine oxygen.

Figure 1 shows pH-rate profiles for the reaction of $\mathbf{1}\cdot\text{H}^+$ with 0.5 M (total) hydroxylamine and with its *N*-methyl and *N,N*-dimethyl derivatives over a range which includes the $\text{p}K_{\text{a}}$ values of both the nucleophile and substrate. The curves follow the expected bell shape below pH 8, with rate maxima in the region where the hydroxylamine is present in the free base form and the substrate as the conjugate acid $\mathbf{1}\cdot\text{H}^+$. The measurements for NH_2OH were extended to higher pH and show in addition the reaction of the anion NH_2O^- with the neutral substrate $\mathbf{1}$, which has no assistance from a general acid. The pH-rate constant profiles were fitted to eq i, where k_0 is the rate constant for the water reaction, k_2 is the second-order rate constant for the reaction of $\mathbf{1}\cdot\text{H}^+$ with the neutral hydroxylamine, and $\chi_{\text{R},\text{NHOH}}$ and $\chi_{\text{+}}$ are the mole fractions of the two reactive species.

- (9) Lewis, R. E.; Neverov, A. A.; Brown, R. S. *Org. Biomol. Chem.* **2005**, *3*, 4082–4088.
 (10) Domingos, J. B.; Longhinotti, E.; Brandao, T. A. S.; Bunton, C. A.; Santos, L. S.; Eberlin, M. N.; Nome, F. *J. Org. Chem.* **2004**, *69*, 6024–6033.
 (11) Domingos, J. B.; Longhinotti, E.; Bunton, C. A.; Nome, F. *J. Org. Chem.* **2003**, *68*, 7051–7058.

- (12) Stanbury, D. M. *Inorg. Chem.* **1991**, *30*, 1293–1296.
 (13) Durckheimer, W. *Liebigs Ann. Chim.* **1969**, *721*, 240–243.
 (14) Carey, F. A.; Sundberg, R. J. *Advanced Organic Chemistry, Part B*; Plenum Press: New York, 1991; p 231.
 (15) Kirby, A. J.; Souza, B. S.; Medeiros, M.; Priebe, J. P.; Manfredi, A.; Nome, F. *J. Chem. Soc., Chem. Commun.* **2008**, 4428–4429.

Table 1. Rate Constants and pK_a Values for the Reaction of Selected Nucleophiles with the Triester $\mathbf{1}\cdot\mathbf{H}^+$ at 60 °C and an Ionic Strength of 1.0 M (KCl)

nucleophile	pK_a	$\log k_2/\text{M}^{-1} \text{s}^{-1}$	$k_2/\text{M}^{-1} \text{s}^{-1}$
H ₂ O	-1.74	-5.80	1.58×10^{-6a}
H ₂ PO ₄ ⁻	1.90	-3.82	0.000151^a
HCOO ⁻	3.53	-2.69	0.00204^a
MeCOO ⁻	4.52	-2.62	0.00240^a
HPO ₄ ²⁻	6.51	-1.70	0.0200^a
NH ₂ OH ^b	6.04	0.121	1.32
CH ₃ NHOH	6.23	0.470	2.95
(CH ₃) ₂ NOH	5.45	-0.446	0.358
Me ₃ N ⁺ -O ⁻	4.99		<i>c</i>
CH ₃ ONH ₂	4.62		<i>c</i>
CF ₃ CH ₂ NH ₂	4.86	-2.63	0.00234
imidazole	7.02	-0.821	0.151

^a From ref 1. ^b For the reaction of NH₂O⁻ with neutral triester **1**, $k_2 = (3.32 \pm 0.39) \times 10^{-3} \text{ M}^{-1} \text{ s}^{-1}$. ^c Too slow to measure (pK_a values from ref 2).

[R,R'NOH_{tot}] represents the total concentration, here 0.5 M, of the hydroxylamine plus its conjugate acid. In practice catalysis by hydroxylamine is strong enough that the contribution from the hydrolysis reaction (see Figure 1) is not significant at most pH values.

$$k_{\text{obsd}} = (k_0 + k_2[\text{RR}'\text{NOH}_{\text{tot}}] \cdot \text{R,R}'\text{NOH}) \cdot \chi_+ \quad (\text{i})$$

Least-squares fits to eq i give the second-order rate constants for the reactions of the hydroxylamine free bases with $\mathbf{1}\cdot\mathbf{H}^+$ shown in Table 1, which also shows the (kinetic) pK_a values derived for the hydroxylamines at 60 °C and, for comparison, data for the reactions with oxygen nucleophiles reported previously.¹ Significantly, the reaction of methoxyamine, also an α -effect nucleophile, was too slow to measure. The pK_a of the dimethylammonium group of the substrate was shown previously to be 4.63 at 60 °C.¹

The observed small differences in reactivity between the hydroxylamines follow the changes in their apparent basicities, as observed generally for secondary > primary > tertiary amines,¹⁶ and are observed also for the reactions of hydroxylamines with phosphate di- and monoesters **3** and **4**.^{2,3} The hydroxylamines are, also typically, significantly more reactive than other oxygen or nitrogen nucleophiles of similar basicity, as illustrated by the Brønsted plot of Figure 2 and the data in Table 1. We could detect no significant reaction with methoxyamine, which, consistently, reacted 54 times more slowly than hydroxylamine with the diester $\mathbf{3}\cdot\mathbf{H}^+$; differences are evidently greater for the triester reactions with nucleophiles.

The sensitivity of the rates to the basicity of the nucleophile, as measured by the Brønsted slope β_{nuc} , is 0.50 ± 0.04 for the series of oxygen nucleophiles measured previously,¹ but apparently much greater ($\beta_{\text{nuc}} = 1.12 \pm 0.17$) for the three hydroxylamines—albeit over a very restricted range of pK_a . This high figure is consistent with a parallel set of experiments we have performed with the neutral triester diethyl 2,4-dinitrophenyl phosphate (which has reactivity similar to that of $\mathbf{1}\cdot\mathbf{H}^+$), where the Brønsted slope for the reactions with the three hydroxylamines was the same (1.135 ± 0.040 ; see Figure S.3, Supporting Information) within experimental error. Similar but smaller effects can be perceived in the reactions of the hydroxylamines with the di- and monoesters **3** and **4**.^{2,3}

These figures must be interpreted with care, because the apparent pK_a values used (Table 1) are global figures, containing

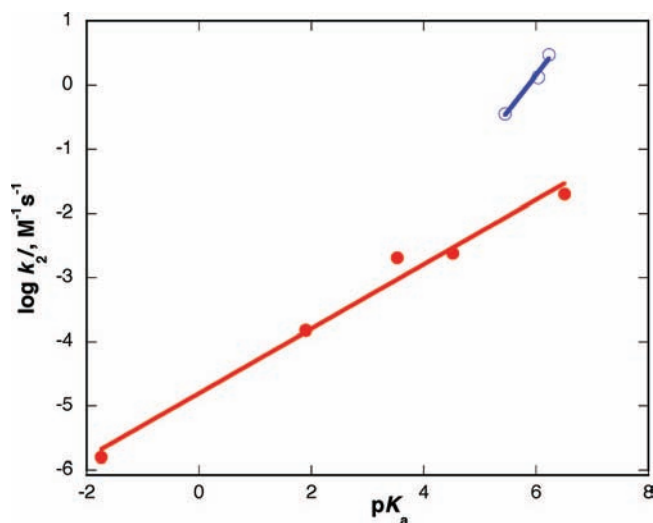


Figure 2. Brønsted plot comparing second-order rate constants for the reactions of $\mathbf{1}\cdot\mathbf{H}^+$ with NH₂OH, MeNHOH, and Me₂NOH (open circles) with those for its reactions with oxygen nucleophiles (closed circles) given in Table 1. The slopes are 1.12 ± 0.17 and 0.50 ± 0.04 , respectively.

undefined but almost certainly unequal contributions from the ionizations of the OH and NH⁺ groups of the hydroxylammonium conjugate acids of the nucleophiles (and in some cases perhaps also contributions from nitrogen attack, though in the case of the triester oxygen attack appears to be quantitative in terms of the products from the diimide route). However, if the microscopic pK_a of the OH group is significantly higher than the apparent value used in the Brønsted plot, the observed rate constant must be corrected by a similar factor to account for the lower concentration of the NH₃⁺-O⁻ form present, with the result that the slope of the plot is not affected. A possible alternative explanation is that the high slope is exaggerated by steric effects, reducing significantly the rate of nucleophilic attack by Me₂NOH or Me₂NH⁺O⁻ on the (EtO)₂P(O)⁻ center.

Such high sensitivity to the basicity of the hydroxylamine has not been observed previously and could be interpreted in terms of a significantly greater amount of bond formation to the nucleophile in the transition state, bringing this closer to the pentacovalent addition intermediate. At this stage it appears that the effect is specific to hydroxylamines with free OH groups, since the Brønsted slopes observed for a different (non-hydroxylamine) set of α -effect nucleophiles with diethyl *p*-nitrophenyl phosphate are slightly lower than those measured for reactions with other (oxyanion) nucleophiles.¹⁷ This, together with the significantly lower reactivity of NH₂OMe, is further evidence consistent with a different mechanism for the attack of the hydroxylamines R,R'NOH, which we suggest involves the zwitterionic ammonia oxide form.

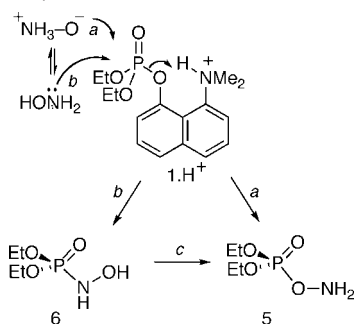
We now have good chemical evidence, discussed above, that hydroxylamine is phosphorylated on oxygen in its reactions with activated phosphate triesters. The remaining question is whether the diethyl phosphate intermediate **5** is formed directly (path a in Scheme 4) or by rearrangement of the first-formed *N*-hydroxyphosphoramidate **6** (Scheme 4, path b). Such a rearrangement (c) is precedented,¹⁸ though not apparently observed for **6** (and certainly not rapidly enough to account for our

(16) Jencks, W. P. *Catalysis in Chemistry and Enzymology*; McGraw-Hill: New York, 1969.

(17) Simanenkov, Y. S.; Popov, A. F.; Prokop'eva, T. M.; Karpichev, E. A.; Savelova, V. A.; Suprun, I. P.; Bunton, C. A. *Russ. J. Org. Chem.* **2002**, *38*, 1286–1298.

(18) Mahajna, M.; Casida, J. E. *Chem. Res. Toxicol.* **1998**, *11*, 26–34.

Scheme 4. Two Possible Routes for the Formation of the O-Phosphorylated Hydroxylamine **5**, Which Reacts Further As Shown (for NH_2OX) in Scheme 3^a



^a The evidence (and Occam's razor) favor the direct path a.

observations).¹⁹ It would be much slower for the corresponding product from a diester and especially a monoester and is ruled out for the corresponding reactions with activated carboxylic acids, which give the stable hydroxamic acids. The evidence is thus consistent with direct attack by oxygen for all these reactions, unambiguously in most cases but not conclusively for the phosphate triesters studied in this work. Since the triesters with the “hardest” phosphorus centers have the most to gain thermodynamically by the initial formation of the P–O rather than a P–N bond, our working hypothesis is that the reaction of hydroxylamine with $1\cdot\text{H}^+$ involves the $\text{S}_{\text{N}}2(\text{P})$ displacement of the naphtholate oxygen by ammonia oxide (Scheme 4, path a) coupled with its protonation by the neighboring dimethylammonium group, acting as a highly efficient general-acid catalyst.

Calculations and the Mechanism of the Hydroxylamine Reaction. Computationally we could find the transition-state structure for route a of Scheme 4 without difficulty, but efforts to obtain a transition structure for route b failed, all attempts indicating only repulsive interactions. The unique transition-state structure obtained for nucleophilic attack by ammonia oxide on the triester $1\cdot\text{H}^+$ (Figure 3) shows a well-defined trigonal bipyramidal arrangement of oxygen atoms around the phosphorus center, with the oxygens of the incoming nucleophile and the leaving group in the expected axial positions.

The structure shown in Figure 3 clearly represents the transition state for the *formation* of the pentacoordinate addition intermediate: the bond to the leaving group is lengthened by just 7%, not a great deal shorter—1.714 Å compared with 1.782 Å—than the developing bond to the incoming nucleophile, but approaching the length expected for this bond in the pentacoordinate addition intermediate. [Few phosphorane crystal structures are available with an axial OAr and at least two O–alkyl bonds, but we have reported a P–OAr bond length of 1.738 Å in one such case (Jones, P. G.; Kirby, A. J.; Pilkington, M. *Acta Crystallogr., E*, **2002**, 58, o268–o269).] Consistently, the hydrogen bond supporting intramolecular general-acid catalysis of bond breaking has developed only slightly, with $\text{O}_{\text{LG}}\cdots\text{N} = 2.627$ Å, the OHN bond angle equal to 144.8°, and the proton just 0.2° out of plane, compared with values of $\text{O}_{\text{LG}}\cdots\text{N} = 2.696$

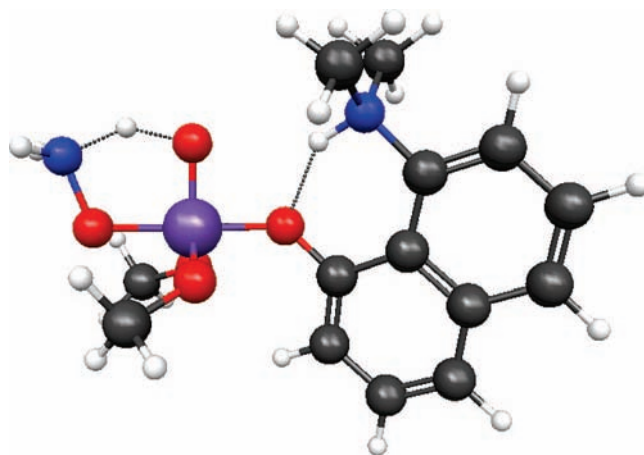


Figure 3. Transition-state structure for nucleophilic attack by ammonia oxide on the triester $1\cdot\text{H}^+$, calculated using GAMESS²⁰ at the 6-31G(d,p) restricted Hartree–Fock level, using the C-PCM model for solvation (see Table S.6, Supporting Information) (figure and postcalculation analysis made using MacMolPlt²¹). Note the two key hydrogen bonds.

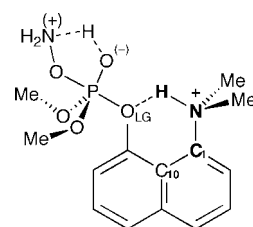


Figure 4. $\text{N}^+\text{H}\cdots\text{O}$ hydrogen bonding in the transition-state structure of Figure 3. H-bonds cannot be linear in five- and six-membered ring systems, but the protons are otherwise almost optimally placed: the dihedral angle $\text{C}(10)\text{--C}(1)\text{--N}^+\text{--H}$ is 0.2°, and one $\text{N}^+\text{--H}$ bond of the ammonia oxide nucleophile is aligned almost coplanar with the developing $\text{P}\text{--O}^-$ bond. See the text.

Å, $\text{OHN} = 140.6^\circ$, and dihedral angle $\text{O}_{\text{LG}}\text{--C}(1)\text{--N}\text{--H} = 11.0^\circ$ in the reactant triester (see Table S.4, Supporting Information), which already shows a weak hydrogen bond to the leaving group oxygen.

Comparison with the TS for the same reaction of the corresponding diester $3\cdot\text{H}^+$ illustrates the differences between associative and more dissociative mechanisms. The P–O distances, 1.782 and 1.714 Å for bond making and bond breaking, respectively, compared with the corresponding values (1.807 and 2.008 Å) for the same reaction of the diester $3\cdot\text{H}^+$,² show the departure of the leaving group significantly less advanced for the reaction of the triester. Consistent with this, the hydrogen bond supporting intramolecular general-acid catalysis is slightly longer and thus weaker: the distance $\text{O}_{\text{LG}}\cdots\text{N}$ is 2.627 Å, the OHN bond angle 144.8°, and the proton just 0.2° out of plane, as discussed above; the corresponding values for the diester are 2.609 Å, 150.2°, and 3.5°. (The structure calculated under the same conditions for the triester reactant shows a weak hydrogen bond to the leaving group oxygen, with a dihedral angle $\text{O}_{\text{LG}}\text{--C}(1)\text{--N}\text{--H}$ of 0.7° (see Table S.4, Supporting Information).

The most striking feature of the TS structure is the proton transfer from the NH_3^+ group of the ammonia oxide nucleophile to the phosphoryl oxygen of the triester. The proton is in-flight in the transition state (Figures 3 and 4), with the proton almost equidistant (1.238 and 1.211 Å) between the donor and acceptor atoms, indicating that the proton transfer—concerted but presumably not synchronous with the changes in bonding between

(19) Ware, R. W.; King, S. B. *J. Org. Chem.* **2000**, 65, 8725–8729.

(20) Schmidt, M. W.; Baldrige, K. K.; Boatz, J. A.; Elbert, S. T.; Gordon, M. S.; Jensen, J. H.; Koseki, S.; Matsunaga, N.; Nguyen, K. A.; Su, S. J.; Windus, T. L.; Dupuis, M.; Montgomery, J. A. *J. Comput. Chem.* **1993**, 14, 1347–1363.

(21) Bode, B. M.; Gordon, M. S. *J. Mol. Graphics Modell.* **1998**, 16, 133–138.

(22) Bourne, N.; Williams, A. *J. Am. Chem. Soc.* **1984**, 106, 7591–7596.

heavy atoms—marks the top of the barrier. This is equally true for the reaction of the diester,² where the proton is again almost equidistant (1.233 and 1.221 Å) between donor N⁺ and acceptor O⁻ (only one of the two negatively charged oxygens is involved). The nucleophile behaves in much the same way in the two reactions: apart from the in-flight proton, the N⁺···O distance across the hydrogen bond is 2.316 Å and the angle N⁺HO 142.0° for the triester, compared with 2.330 Å and 143.5° for the diester TS, and the length of the developing O···P bond is almost the same (triester, 1.782 Å; diester, 1.807 Å) in the two cases. However, the consequent increase in negative charge density on the phosphorane is evidently harder to accommodate for the anionic diester, so that bond breaking is already under way and the concerted process more dissociative.

Conclusions

Intramolecular general-acid catalysis is highly efficient (supporting rate accelerations or effective molarities of 10⁵–10⁶)⁵ in only a handful of model systems, all involving reactions in which a strong intramolecular hydrogen bond is formed. 8-(*N,N*-dimethylamino)-1-naphthol (**2**), as a leaving group stabilized by a strong intramolecular hydrogen bond (the p*K*_a of the OH group is 14.9²³), elicits rate accelerations of this same order of magnitude for the attack of nucleophiles on the phosphate mono-, di-, and triesters **4**·H⁺, **3**·H⁺, and **1**·H⁺, despite the presence of significant intramolecular hydrogen bonding from the catalytic dimethylammonium group to the leaving group oxygen in the reactant diester **3**·H⁺ and especially the monoester **4**·H⁺. Since catalytic efficiency depends on the differential stabilization of the transition vs ground state, these similarities may seem surprising. However, strong hydrogen bonding to the leaving group oxygen of a phosphate monoester

dianion is expected (from calculations³ and related crystal structure measurements^{24,25}) to lengthen and thus weaken the scissile P–O bond, such electrostatic interactions providing “a common driving force underlying both bond lengthening and observed rate increases”.²⁶ Thus, compared with a similar ester lacking the neighboring general acid, the scissile P–O bond is weakened by both ground-state and transition-state effects in the case of the phosphate monoester “dianion” **4**·H⁺, but by transition-state effects almost exclusively in the case of the triester **1**·H⁺, with the reaction of the diester **3**·H⁺ lying in between.

Finally, our results confirm that the reaction of the triester **1**·H⁺ with hydroxylamine gives the O-phosphorylated product, and our calculated transition state for the reaction is consistent with an explanation for the high rate of the reaction in terms of nucleophilic attack by ammonia oxide assisted by proton transfer catalysis by its NH₃⁺ group.

Acknowledgment. We are grateful to Capes, PRONEX, CNPq, and FAPESC (Brazil) for their support of this work. M.F.L. thanks CNPq for a fellowship.

Supporting Information Available: Spectra supporting structural assignments for diimide reduction products, kinetic data for reactions of hydroxylamines with triester **1**·H⁺ in water at 60 °C and an ionic strength of 1.0 M (KCl) as a function of the pH and temperature, and Cartesian coordinates for calculated (C-PCM-HF 6-31G(d,p)) structures of triester **1**·H⁺ and ammonia oxide and the transition state for the reaction between them. This material is available free of charge via the Internet at <http://pubs.acs.org>.

JA808746F

- (23) Awwal, A.; Hibbert, F. *J. Chem. Soc., Perkin Trans. 2* **1977**, 152–156.
(24) Brandao, T. A. S.; Orth, E. S.; Rocha, W. R.; Bortoluzzi, A. J.; Bunton, C. A.; Nome, F. *J. Org. Chem.* **2007**, *72*, 3800–3807.

- (25) Jones, P. G.; Kirby, A. J. *J. Am. Chem. Soc.* **1984**, *106*, 6207–6212.
(26) Cheng, H.; Nikolic-Hughes, I.; Wang, J. H. H.; Deng, H.; O'Brien, P. J.; Wu, L.; Zhang, Z. Y.; Herschlag, D.; Callender, R. *J. Am. Chem. Soc.* **2002**, *124*, 11295–11306.